

This article was downloaded by:

On: 27 January 2011

Access details: *Access Details: Free Access*

Publisher *Taylor & Francis*

Informa Ltd Registered in England and Wales Registered Number: 1072954 Registered office: Mortimer House, 37-41 Mortimer Street, London W1T 3JH, UK



Phosphorus, Sulfur, and Silicon and the Related Elements

Publication details, including instructions for authors and subscription information:

<http://www.informaworld.com/smpp/title~content=t713618290>

Synthesis, Crystal Structure, and Conductivity Investigation of a New Monophosphate: $(2\text{-CH}_3\text{OC}_6\text{H}_4\text{CH}_2\text{NH}_3)\text{H}_2\text{PO}_4$

H. Dhaouadi^a; H. Marouani^a; M. Rzaigui^a; A. Madani^b

^a Faculté des Sciences, Laboratoire de Chimie des Matériaux, Zarzouna, Bizerte, Tunisie ^b Faculté des Sciences, Laboratoire de Physique des Matériaux, Zarzouna, Bizerte, Tunisie

To cite this Article Dhaouadi, H. , Marouani, H. , Rzaigui, M. and Madani, A. (2006) 'Synthesis, Crystal Structure, and Conductivity Investigation of a New Monophosphate: $(2\text{-CH}_3\text{OC}_6\text{H}_4\text{CH}_2\text{NH}_3)\text{H}_2\text{PO}_4$ ', *Phosphorus, Sulfur, and Silicon and the Related Elements*, 181: 8, 1801 – 1814

To link to this Article: DOI: 10.1080/10426500500538750

URL: <http://dx.doi.org/10.1080/10426500500538750>

PLEASE SCROLL DOWN FOR ARTICLE

Full terms and conditions of use: <http://www.informaworld.com/terms-and-conditions-of-access.pdf>

This article may be used for research, teaching and private study purposes. Any substantial or systematic reproduction, re-distribution, re-selling, loan or sub-licensing, systematic supply or distribution in any form to anyone is expressly forbidden.

The publisher does not give any warranty express or implied or make any representation that the contents will be complete or accurate or up to date. The accuracy of any instructions, formulae and drug doses should be independently verified with primary sources. The publisher shall not be liable for any loss, actions, claims, proceedings, demand or costs or damages whatsoever or howsoever caused arising directly or indirectly in connection with or arising out of the use of this material.

Synthesis, Crystal Structure, and Conductivity Investigation of a New Monophosphate: $(2\text{-CH}_3\text{OC}_6\text{H}_4\text{CH}_2\text{NH}_3)\text{H}_2\text{PO}_4$

H. Dhaouadi

H. Marouani

M. Rzaigui

Laboratoire de Chimie des Matériaux, Faculté des Sciences, Zarzouna, Bizerte, Tunisie

A. Madani

Laboratoire de Physique des Matériaux, Faculté des Sciences, Zarzouna, Bizerte, Tunisie

Chemical preparation, crystal structure, thermogravimetric and differential analysis, solid state ^{31}P MAS NMR characterization, and IR spectroscopic investigations are given for a new organic cation dihydrogenmonophosphate, $(2\text{-CH}_3\text{OC}_6\text{H}_4\text{CH}_2\text{NH}_3)\text{H}_2\text{PO}_4$. This compound is monoclinic $\text{C2}/c$, with unit cell parameters $a = 27.740(8)$, $b = 4.827(2)$, $c = 16.435(3)$ Å, $\beta = 93.79(2)^\circ$, $V = 2196(1)$ Å³, $Z = 8$, and $\rho = 1.422$ g · cm⁻³. The crystal structure has been determined and refined to $R = 0.046$ ($R_w = 0.056$), using 1,746 independent reflections with $I > 3\sigma(I)$. Its atomic arrangement can be described by infinite polyanions $[\text{H}_2\text{PO}_4]_n^{n-}$, organized in ribbons alternating with organic cations. Strong hydrogen bonds connect the different components. Electrical conductivity measurements show that the $[2\text{-CH}_3\text{OC}_6\text{H}_4\text{CH}_2\text{NH}_3]\text{H}_2\text{PO}_4$ has a low ionic conductivity value at 403 K.

Keywords Electric conductivity; hydrogen bonds; IR spectroscopy; layered compounds; NMR spectroscopy; X-ray diffraction

INTRODUCTION

Inorganic–organic hybrid compounds have been of great interest over recent years from both an academic and industrial point of view¹ due to their vast structural and compositional diversities. Among these materials, organic phosphates are particularly interesting. It has been found that hydrogen bonds and the nature of organic molecules seem to determine the molecular organization of these compounds as to build

Received August 1, 2005; accepted September 22, 2005.

Address correspondence to H. Dhaouadi, Laboratoire de Chimie des Matériaux, Faculté des Sciences, Zarzouna, Bizerte, 7021 Tunisie. E-mail: mohamed.tzaigui@fsb.rnu.tn

infinite anionic networks with various geometries: ribbons,² chains,³ two-dimensional networks,⁴ and three-dimensional networks.⁵ In order to study the influence on the chemical and structural features of hydrogen bonds, we report and discuss in the present work results of a structural investigation concerning a new organic-cation monophosphate, $[2\text{-CH}_3\text{OC}_6\text{H}_4\text{CH}_2\text{NH}_3]\text{H}_2\text{PO}_4$. This compound is characterized by IR spectroscopy, differential thermal analysis, ^{31}P and ^{13}C solid state NMR spectroscopy, and ionic conductivity.

RESULTS AND DISCUSSION

Crystal Structure

Final atomic coordinates of $(2\text{-CH}_3\text{OC}_6\text{H}_4\text{CH}_2\text{NH}_3)\text{H}_2\text{PO}_4$ and their B_{eq} (B_{iso} for hydrogen atoms) are given in Table I. Main geometrical features of different entities are indicated in Table II.

The asymmetric unit of the dihydrogenmonophosphate is shown in the ORTEP drawing with a 50% probability of thermal ellipsoids in Figure 1.

The only P atom is tetrahedrally coordinated to four distinct oxygen atoms, O1, O2, O3, and O4. Among the four oxygen atoms, two of the coordinating oxygen are attributed to doubly bonded oxygen atoms, while the two other ones ($d(\text{P-O1}) = 1.540(2) \text{ \AA}$ and $d(\text{P-O2}) = 1.559(2) \text{ \AA}$) correspond to the P-OH bonds. The average values for the P-O distances and O-P-O angles are 1.521 \AA and 109.415° , respectively. These values are in excellent agreement with those relative to the protonated oxoanions.⁶ It is worth-noting that the $\text{O} \cdots \text{O}$ distances involved in the hydrogen bonds ($2.570(2)\text{--}2.534(3) \text{ \AA}$) are of the same order of magnitude as the $\text{O} \cdots \text{O}$ distances in the H_2PO_4 tetrahedron [$2.523(2)\text{--}2.404(3) \text{ \AA}$]. These distances and the short $\text{P} \cdots \text{P}$ one of $4.247(1) \text{ \AA}$ allow us to consider the $[\text{H}_2\text{PO}_4]_n^{n-}$ network as a polyanion.

Figure 2 displays the crystal structure viewed along the *b* direction. This projection shows that the inorganic entities form ribbons located at $z = \frac{1}{4}$ and $z = \frac{3}{4}$. Between these ribbons the organic molecules are trapped to establish the three-dimensional network stability via various interactions (electrostatic, H-bonds, Van der Waals).

Hydrogen bonding has a key role in linking the template molecules with the anionic ribbons made by H_2PO_4 moieties. All the D(donor)-H \cdots A(acceptor) hydrogen bonds are listed in Table III, with an upper limit of $2.30(3) \text{ \AA}$ for H \cdots A distances and a lower limit of $144(2)^\circ$ for D-H \cdots A bond angles. Thus, this atomic arrangement exhibits two types of hydrogen bonds: O(P)-H \cdots O involving two short contacts with H \cdots O of $1.77(3)$ and $1.78(4) \text{ \AA}$ ensures the cohesion between PO_4

TABLE I Final Atomic Coordinates and B_{eq.} for the non Hydrogen Atoms (B_{iso.} for Hydrogen Atoms). Esd. are Given in Parentheses. B_{eq.} = 4/3 $\sum_i \sum_j \beta_{ij} \cdot a_i \cdot b_j$.

Atoms	x (σ)	y (σ)	z (σ)	B _{eq.} (\AA^2)
P(1)	0.53365(2)	0.1168(1)	0.36987(3)	2.840(9)
O(1)	0.56287(5)	0.1160(5)	0.2934(1)	6.06(4)
O(2)	0.55730(6)	-0.1037(3)	0.4292(1)	4.61(3)
O(3)	0.54009(7)	0.3825(3)	0.4148(1)	5.07(4)
O(4)	0.48175(5)	0.0471(3)	0.34725(8)	3.77(3)
O(5)	0.64946(6)	0.3423(4)	0.49300(9)	5.01(4)
N(1)	0.56229(6)	0.4013(4)	0.5844(1)	3.49(4)
C(1)	0.60715(8)	0.4905(5)	0.6309(2)	4.13(5)
C(2)	0.64628(7)	0.2738(4)	0.6319(1)	3.28(4)
C(3)	0.66710(7)	0.2039(5)	0.5603(1)	3.57(4)
C(4)	0.70311(8)	0.0057(6)	0.5615(2)	4.67(5)
C(5)	0.71882(8)	-0.1170(6)	0.6338(2)	5.19(6)
C(6)	0.69904(9)	-0.0484(5)	0.7043(2)	5.01(6)
C(7)	0.66261(8)	0.1464(5)	0.7033(1)	4.16(5)
C(8)	0.6635(1)	0.254(1)	0.4160(2)	6.80(8)
				B _{iso.} (\AA^2)
H(O1)	0.5482(9)	0.067(5)	0.251(2)	5.9(6)
H(O2)	0.553(1)	-0.257(8)	0.408(2)	8.8(9)
H(1N)	0.5668(8)	0.380(5)	0.529(2)	5.2(6)
H(2N)	0.5413(8)	0.529(5)	0.590(1)	4.7(5)
H(3N)	0.5502(7)	0.248(5)	0.605(1)	4.2(5)
H(1C1)	0.6138(9)	0.638(5)	0.602(1)	5.5(6)
H(2C1)	0.5987(8)	0.528(5)	0.682(1)	4.4(5)
H(C4)	0.7173(9)	-0.023(5)	0.513(2)	5.6(6)
H(C5)	0.7460(9)	-0.251(6)	0.632(1)	5.5(6)
H(C6)	0.7083(9)	-0.129(5)	0.752(2)	5.6(6)
H(C7)	0.6486(7)	0.198(5)	0.752(1)	3.9(5)
H(1C8)	0.6995(9)	0.282(6)	0.411(2)	6.8(7)
H(2C8)	0.654(1)	0.048(7)	0.403(2)	7.7(8)
H(3C8)	0.6464(9)	0.374(5)	0.382(2)	5.5(6)

tetrahedron to build the ribbons, whereas N-H \cdots O, including three distances with H \cdots O values in the range 1.88(3)–2.30(3) Å, links parallel ribbons.

Regarding the organic cations arrangement, the protonated 2-methoxybenzyl amine molecule is localized in the interlayer spacing and neutralizes the negative charge of the anionic part. These groups are organized in opposition, thus creating a local inversion center. Such a situation is not favorable to the non centrosymmetrical arrangement

TABLE II Main Interatomic Distances (Å) and Angles (°) in (2-CH₃O)C₆H₄NH₃)H₂PO₄ Atomic Arrangement. Estimated Standard Deviations are Given in Parentheses

P	The PO ₄ Tetrahedron			
	O(1)	O(2)	O(3)	O(4)
O(1)	1.540(2)	2.486(3)	2.490(3)	2.494(2)
O(2)	106.7(1)	1.559(2)	2.404(3)	2.523(2)
O(3)	110.8(1)	104.3(1)	1.485(2)	2.497(3)
O(4)	110.20(1)	111.0(1)	113.5(1)	1.501(2)
O(1)-H(O1)	0.81(3) Å		P-O(1)-H(O1)	116(2)°
O(2)-H(O2)	0.82(4) Å		P-O(2)-H(O2)	108(3)°
(2-CH₃OC₆H₄NH₃)⁺ group				
N-C(1)		1.481(3)	N(1)-C(1)-C(2)	112.6(2)
C(1)-C(2)		1.507(4)	C(1)-C(2)-C(3)	120.0(2)
C(2)-C(3)		1.387(3)	C(2)-C(3)-C(4)	119.8(2)
C(3)-C(4)		1.382(4)	C(3)-C(4)-C(5)	120.0(3)
C(4)-C(5)		1.372(5)	C(4)-C(5)-C(6)	120.8(3)
C(5)-C(6)		1.356(5)	C(5)-C(6)-C(7)	119.6(3)
C(6)-C(7)		1.380(4)	C(6)-C(7)-C(2)	121.0(3)
C(7)-C(2)		1.375(4)	C(7)-C(2)-C(3)	118.9(2)
C(3)-O(5)		1.355(3)	C(7)-C(2)-C(1)	121.1(2)
O(5)-C(8)		1.414(4)	C(3)-O(5)-C(8)	118.4(3)
			C(2)-C(3)-O(5)	115.1(2)
			C(4)-C(3)-O(5)	125.1(2)

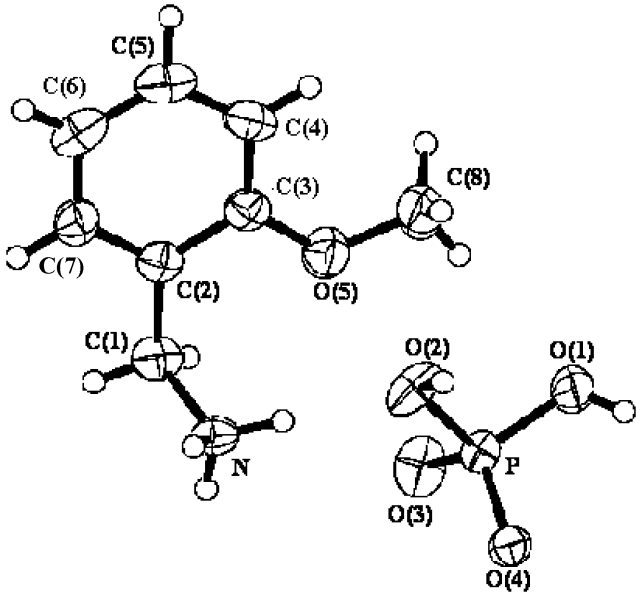


FIGURE 1 ORTEP view of the structure of (2-CH₃OC₆H₄CH₂NH₃)H₂PO₄ (50% thermal ellipsoids).

TABLE III Hydrogen Bonds Geometry: Bond Lengths (Å) and Angles (°)

D - H···A	D···A	D-H	H···A	D-H···A
O(1)-H(O1)···O(4)	2.570(2)	0.81(3)	1.77(3)	166(3)
O(2)-H(O2)···O(3)	2.534(3)	0.82(4)	1.78(3)	151(4)
N-H(1N)···O(3)	2.817(3)	0.93(3)	1.97(3)	150(2)
N-H(2N)···O(3)	3.027(3)	0.85(3)	2.30(3)	144(2)
N-H(3N)···O(4)	2.761(3)	0.89(3)	1.88(3)	173(3)

that we try to elaborate. Each organic entity is bounded to two different (H₂PO₄)⁻ groups belonging to two different phosphoric ribbons through three N-H···O hydrogen bonds. The organic molecule exhibits a regular spatial configuration with usual distances C-C, C-N, and C-O and angles C-C-C, C-C-N, and C-O-C. Interatomic distances and bond angles in this organic group are reported in Table II. The aromatic ring has a good coplanarity with an average deviation of $d = 0.0036$ Å. The mean value of the (C-C) length of the benzene cycle is 1.375(4) Å, which is between a single bond and a double bond and agrees with that in

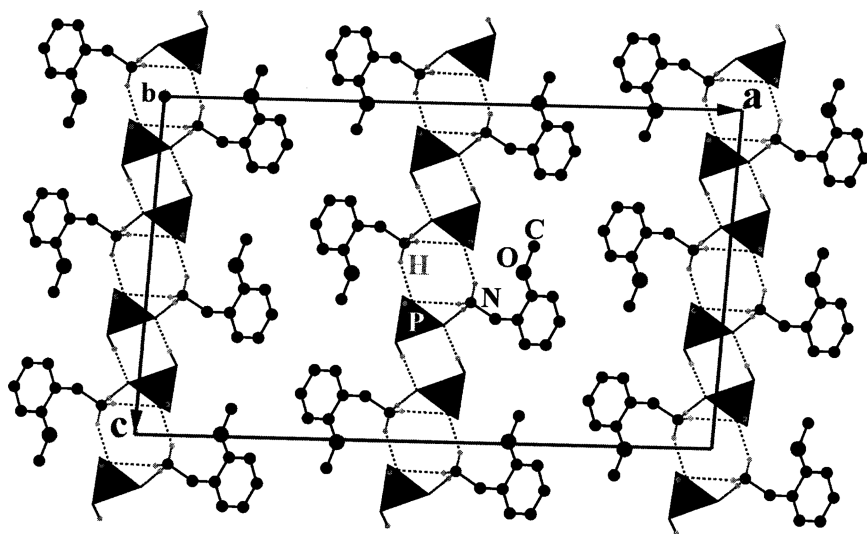


FIGURE 2 Projection of the atomic arrangement of (2-CH₃OC₆H₄CH₂NH₃)H₂PO₄ along the b-axis. The phosphoric groups are given in the tetrahedral representation. The smaller dotted circles represent the hydrogen atoms. The other atoms are indicated by their symbols. Intermolecular H-bonds are denoted by dotted lines.

benzene.⁷ Furthermore, the distances of C(1)-C(2), N-C(1)[1.507(4) Å, and 1.481(3) Å] clearly indicate two single bonds.

The coplanar methoxy group with the phenyl ring is characterized by a torsion angle of $-170.6(3)^\circ$. The O(5)-C(3)-C(4) angle ($125.1(2)^\circ$) is larger than the O(5)-C(3)-C(2) angle ($115.1(2)^\circ$); this can be attributed to the establishment of a weak intramolecular hydrogen bond [N-H(1N) \cdots O(5) = 2.944(2) Å, \angle (N-H(1N) \cdots O(5)) = $116.0(2)^\circ$]. Indeed, the tendency of the O(5) atom getting to the H(1N) of the amine group permits us to consider that the O(5) atom accepts the H(1N) as a type of intramolecular hydrogen bond. The formation of this kind of intramolecular hydrogen bond would allow the organic molecule to be highly planar. It is worth noting that this type of hydrogen bond is found in other compounds, such as 4-hydroxy-coumarin.⁸

NMR Spectroscopy

High-resolution NMR spectroscopy is a powerful technique for the characterization of phosphates. From the isotropic chemical shift value, structural aspects have often been studied. Proton decoupled ^{31}P MAS-NMR of crystalline monophosphate $(2\text{-CH}_3\text{OC}_6\text{H}_4\text{CH}_2\text{NH}_3)\text{H}_2\text{PO}_4$ is presented in Figure 3. It exhibits only one sharp peak. The corresponding chemical shift value -1.18 ppm was recorded with respect to an 85%

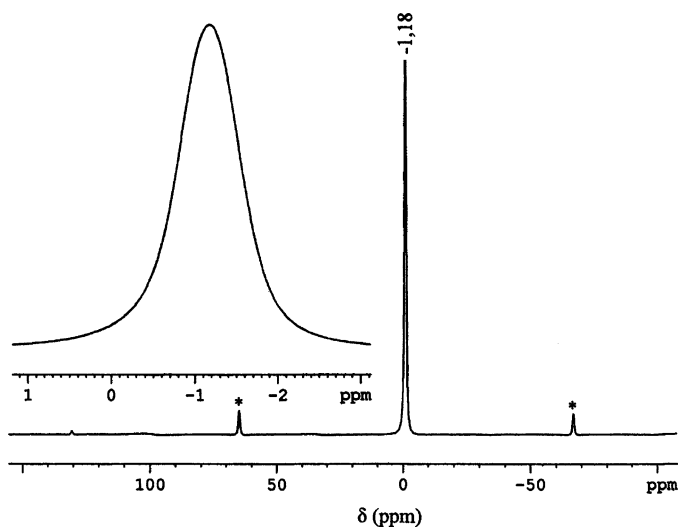


FIGURE 3 The ^{31}P MAS-NMR spectrum of $(2\text{-CH}_3\text{OC}_6\text{H}_4\text{CH}_2\text{NH}_3)\text{H}_2\text{PO}_4$ monophosphate recorded at 4 kHz. * = pinning side bands.

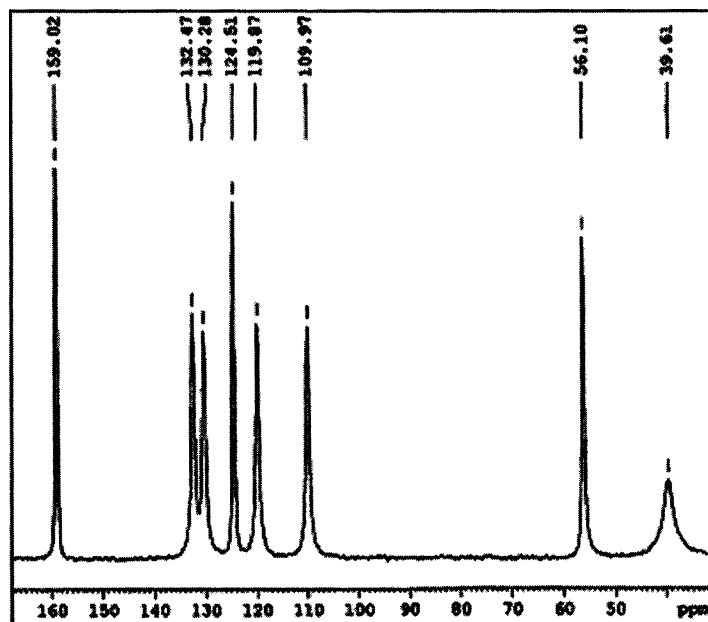
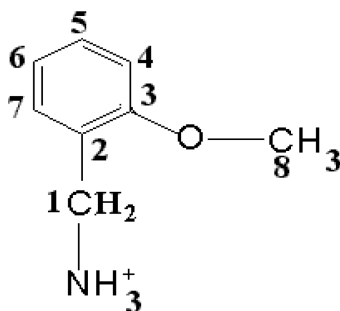


FIGURE 4 The ^{13}C CP-MAS-NMR spectrum of (2-CH₃OC₆H₄CH₂NH₃)-H₂PO₄.

H₃PO₄ aqueous solution. This value agrees with those of the monophosphate (between -10 and $+5$ ppm), depending on the compound.^{9,10} The single isotropic peak observed is related to the number of phosphorus sites.

The ^{13}C CP-MAS NMR spectrum of the title compound given in Figure 4 displays eight resonance peaks corresponding to the different carbon sites. These results are in good agreement with the X-ray structure as only one organic molecule is found in the asymmetric unit. The carbon atoms of the organic group are labeled as depicted in Scheme 1.



SCHEME 1

TABLE IV Calculated and Experimental Chemical Shifts of the Organic Groups Carbon Atoms

Carbon Atoms	C1	C2	C3	C4	C5	C6	C7	C8
δ calculated (ppm)	35.6	123.3	162.7	114.0	126.5	120.7	130.2	56.3
δ experimental (ppm)	39.6	124.5	159.0	109.9	130.3	119.8	132.5	56.1

To assign NMR components to different carbon atoms, we used ChemDrew Ultra 6.0 calculations. The chemical shifts of eight carbon atoms were calculated. The results obtained and the signal attribution are gathered in Table IV.

The results from NMR techniques give a clear evidence for the presence of one organic cation and one phosphorus site in an asymmetric unit of the title compound.

IR Spectroscopy Investigations

The infrared spectrum (Figure 5) of the compound $(2\text{-CH}_3\text{OC}_6\text{H}_4\text{CH}_2\text{NH}_3)\text{H}_2\text{PO}_4$ contains characteristics bands of the 2-methoxybenzylammonium and dihydrogenmonophosphate H_2PO_4^- anions. The

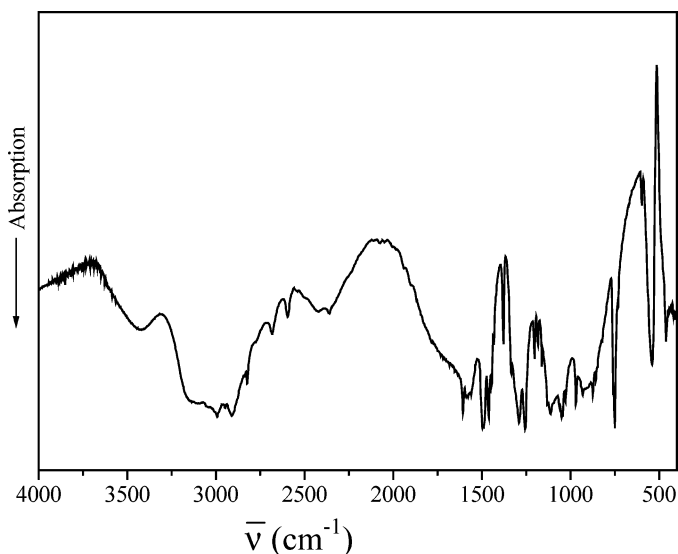


FIGURE 5 The infrared absorption spectrum of $(2\text{-CH}_3\text{OC}_6\text{H}_4\text{CH}_2\text{NH}_3)\text{-H}_2\text{PO}_4$.

stretching and bending modes of the (NH₃⁺) group appear as weak and large bands at 2995 and 1604 cm⁻¹, respectively. They are indicative of the presence of the 2-methoxybenzylammonium molecule in its protonated form.^{11–12} The stretching vibrations of the (-CH₂-) groups appear in the 2900–2583 cm⁻¹ range, and bending modes are observed in the 1500–1461 cm⁻¹ region. The vibrational modes of the PO₄ tetrahedra anions show different groups of bands between 1200–300 cm⁻¹.¹³ In this case, the stretching vibration bands originate from both symmetric ν_1 (A₁), and asymmetric ν_3 (F₂) modes are observed, respectively, in the ranges 1000–800 cm⁻¹ and 1200–1000 cm⁻¹. The bending modes symmetric ν_4 (F₂) and asymmetric ν_2 (E) appear, respectively, in the 650–500 cm⁻¹ and 500–300 cm⁻¹ regions. As in other phosphate groups,^{14–15} the IR bands in the range 2900–2300 cm⁻¹ are assigned to the $\nu_{\text{P-OH}}$, whereas bands observed in the IR spectrum in the 1240–1100 cm⁻¹ region are ascribed to the $\delta_{\text{P-O-H}}$ in plane bending; the $\gamma_{\text{P-O-H}}$ out-of-plane bending modes appear in the range 930–820 cm⁻¹.

Thermal Analysis

The two curves corresponding to differential and thermogravimetric analysis (DTA/TG) under argon flow are given in Figure 6. The DTA curve shows that monophosphate is stable until 484 K, where it undergoes a melting transformation. At the same time, the material begins to undergo a continuous decomposition in a wide temperature range [484–723 K]. The TGA curve undertakes two endothermic weight losses

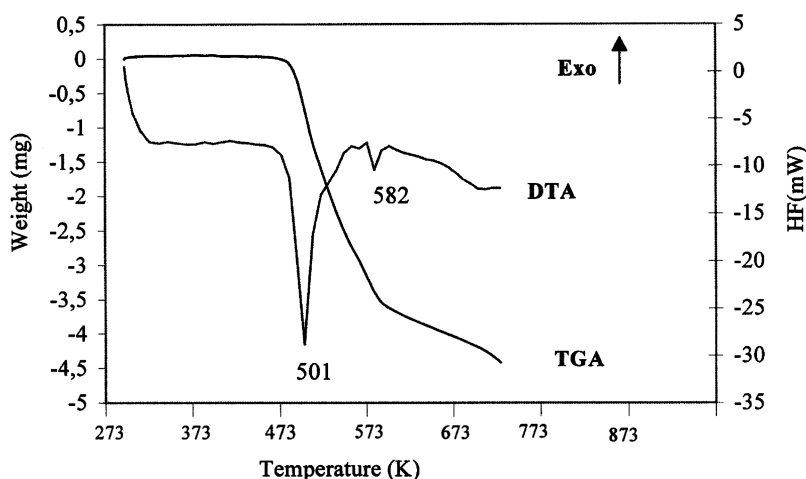
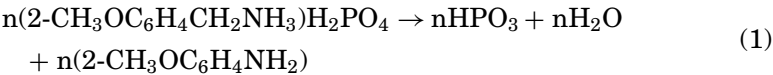


FIGURE 6 DTA and TGA curves of (2-CH₃OC₆H₄CH₂NH₃)H₂PO₄.

in the temperature ranges [503–582 K] and [582–696 K]. The first of these probably corresponds to the progressive pyrolysis of the organic groups. The second endothermic peak centered at 582 K probably corresponds to the removal of water arising from dehydroxylation reactions due to the condensation of two H_2PO_4^- groups, according to Eq. (1):



After heating the sample at 675 K, a black product is obtained containing the residual organic species mixed with the polyphosphoric acid. The DTA curve does not present any peaks before the melting point. This is confirmed by differential scanning calorimetry performed between 300 and 673 K, which does not show any phase transition.

Electrical Conducting Studies

Conductivity measurements lead to the values listed in Table V. The Arrhenius plot of conductivity for $(2\text{-CH}_3\text{OC}_6\text{H}_4\text{CH}_2\text{NH}_3)\text{H}_2\text{PO}_4$ is given in Figure 7. Sample resistance was taken from impedance spectra as the real part of impedance (Z_0). The material displays low conductivity performances as compared to other compounds in Table VI. It is worth noting that the conductivity increases with increasing temperature. We point out that the plot form of $\ln\sigma T$ versus $10^4/T$ is linear with a constant activation energy of 0.25 eV, which agrees with the Arrhenius model of conductivity, $\sigma = \frac{A}{T} \exp(\frac{-E_a}{KT})$ where A is a constant depending on the material, K is the Boltzman constant, and E_a is the activation energy determined by the slope of the interpolating Arrhenius curve, for all investigated temperatures. This seems to indicate only one protonic conductivity mechanism, and there is no modification of

TABLE V Conductivity Result Measurement Values

T(K)	Z_0 (Ω)	σ ($\Omega^{-1}\text{cm}^{-1}$)	$10^4/T$ (K^{-1})	$\ln(\sigma \cdot T)$
292	65641	1.75×10^{-6}	34.25	−7.58
309	45053	2.55×10^{-6}	32.36	−7.15
331	25483	4.51×10^{-6}	30.21	−6.51
348	15755	7.30×10^{-6}	28.73	−5.97
371	9803	11.7×10^{-6}	26.95	−5.44
375	7658	15.0×10^{-6}	26.67	−5.18
396	6884	16.7×10^{-6}	25.25	−5.02
417	5669	20.29×10^{-6}	23.98	−4.77

TABLE VI Conductivity σ ($\Omega^{-1}\text{cm}^{-1}$) and Conduction Activation Energy E_a (eV) of Other Compounds

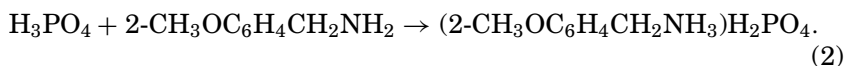
Compounds	Temperature Range (K)	σ ($\Omega^{-1}\text{cm}^{-1}$)	E_a (eV)	Ref.
LiFe ₂ (PO ₄) ₃	400–600	10^2	0.44	16
Na ₃ Sc ₂ (PO ₄) ₃	400–600	5.1×10^{-2}	0.34	16

the electrical proprieties. These results are in good agreement with the calorimetric study, which does not show any phase transition before the melting point.

EXPERIMENTAL

The Synthesis of (2-CH₃OC₆H₄CH₂NH₃)H₂PO₄

Crystals of the title compound were prepared by slowly adding, at r.t., 0.6 cm³ of concentrated orthophosphoric acid (85 wt. %, $d = 1.7$) to an alcoholic solution containing 1.4 cm³ of 2-methoxybenzylamine (98 wt. %, $d = 1.05$). Acid was added until the alcoholic solution became turbid, resulting from Eq. (2):



After filtration, the solution was slowly evaporated at r.t. for several days until the formation of transparent prismatic single crystals of good quality (1.5 g, 60% yield) and suitable dimensions for crystallographic study.

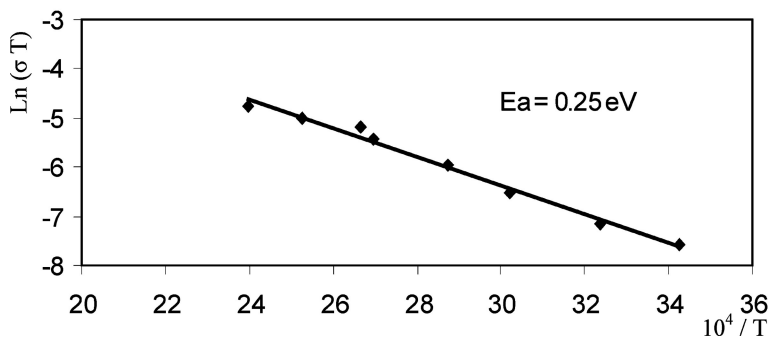


FIGURE 7 The Arrhenius plot of conductivity for (2-CH₃OC₆H₄CH₂NH₃)H₂PO₄.

Chemical synthesis was reproducible, and crystals obtained in this way were stable for a long time under normal conditions of temperature and humidity.

The chemical formula of this new material, 2-methoxybenzyl-ammonium dihydrogenmonophosphate, was determined by X-ray crystal structure analysis.

Characterization Techniques

The title compound has been studied by various physicochemical methods:

X-ray Diffraction

Intensity data collection was performed with a MACH3 Enraf Nonius diffractometer. Experimental parameters used during these measurements, the strategy followed for the structure determination, and its final results are gathered in Table VII.

TABLE VII Crystal Data and Experimental Parameters Used for the Intensity Data Collection Strategy and Final Results of the Structure Determination

Empirical formula	NC ₈ H ₁₄ PO ₅
Formula weight	235.18
Crystal system	monoclinic
Space group	C2/c
a	27.740(8) Å
b	4.827(2) Å
c	16.435(3) Å
β	$\beta = 93.79(2)^\circ$
Z	8
V	2196 (1) Å ³
$\rho_{\text{cal.}}$	1.422 g.cm ⁻³
F(000)	992
$\mu(\text{AgK}\alpha)$	1.37 cm ⁻¹
Crystal size (mm)	(0.11 × 0.03 × 0.015)
Index ranges: $\pm h, k, l$	$h_{\text{max.}} = 41, k_{\text{max.}} = 7, l_{\text{max.}} = 24$
Reflexions collected	4449
Independent reflexions	4321
R _{int}	0.025
Refined parameters	192
R [$I > 3 \sigma(I)$]	0.046
R _(w)	0.056
Goodness of fit	1.409

Crystallographic data for the structure reported in this article have been deposited with the Cambridge Crystallographic Data Center as supplementary publication No. 278690. Copies of the data can be obtained, free of charge, on application to the CCDC, 12 Union Road, Cambridge CB12EZ, UK. E-mail: deposit@ccdc.cam.ac.uk

NMR Spectroscopy

All NMR spectra were recorded on a Bruker DSX-300 spectrometer operating at 121 MHz for ³¹P and 75.49 MHz for ¹³C. The measurements were carried out at r.t. with H₃PO₄(85%) as an external standard reference. The phosphorus spectrum was recorded under classical MAS conditions, while the carbon one was recorded by the use of cross-polarization from protons.

Infrared Spectroscopy

IR spectrum was recorded in the 4000–400 cm⁻¹ range with a Perkin-Elmer FT-IR spectrometer using a sample dispersed in a spectroscopically pure KBr pellet.

Thermal Analysis

Thermal analysis was performed using the multimodule 92 Setaram analyzer operating from r.t. up to 723 K at an average heating rate of 5 K.min⁻¹.

Electrical Conducting Studies

A polycrystalline sample of (2-CH₃OC₆H₄CH₂NH₃)H₂PO₄ was obtained by pressing the crystal powder at 12 ton. Dense pellets suitable for electrophysical measurements were heated at 373 K for 24 h. After heating, pellets were checked by X-ray powder diffraction, which showed that material was chemically stable in this range of temperature. Metallic silver was deposited on both sides, which served as electrodes. The pellet was placed between two blocking electrodes in a tubular furnace and submitted to a temperature regulator.

Conductivity measurements were carried out at r.t. to 403 K with 5–15°C steps by checking the complex impedance spectroscopy with a Hewlett Packard 4129A impedance analyzer. The signal frequency ranged from 10 Hz to 13 MHz.

REFERENCES

- [1] A. K. Cheetham, G. Ferey, T. Loiseau, and T. Angew, *Chem. Int. Ed. Engl.*, **38**, 3268 (1999).
- [2] L. Baouab and A. Jouini, *J. Solid State Chem.*, **141**, 343 (1988).

- [3] M. T. Averbuch-Pouchot and A. Durif, *Acta Cryst.*, **C43**, 1894 (1987).
- [4] M. T. Averbuch-Pouchot, A. Durif, and J. C. Guitel, *Acta Cryst.*, **C44**, 99 (1988).
- [5] M. T. Averbuch-Pouchot, A. Durif, and J. C. Guitel, *Acta Cryst.*, **C45**, 421 (1989).
- [6] G. Ferraris and G. Ivaldi, *Acta Cryst. Sect.*, **B 40**, 1 (1984).
- [7] Z. J. Li, X. M. Chen, Z. X. Ren, Y. Li, X. A. Chen, and Z. T. Huang, *Chinese J. Struct. Chem.*, **16**, 311 (1997).
- [8] L. J. Farrugia, *J. Appl. Cryst.*, **30**, 565 (1997).
- [9] A. R. Grimmer and U. Haubenreisser, *Chem. Phys. Lett.*, **99**, 487 (1983).
- [10] S. Prabhakar, K. J. Rao, and C. N. R. Rao, *Chem. Phys. Lett.*, **139**, 96 (1987).
- [11] A. Gharbi, A. Jouini, M. T. Averbuch-Pouchot, and A. Durif, *J. Solid State Chem.*, **111**, 330 (1994).
- [12] D. Dolphin and A. E. Wick, *Tabulation of Infrared Spectra Data* (John Wiley and Sons, New York, 1977).
- [13] S. Kammoun, M. Kammoun, A. Daouad, and F. Romain, *Spectrochim. Acta*, **47A**, 1051 (1991).
- [14] A. C. Chapman and L. E. Thirlwell, *Spectrochim. Acta*, **20**, 937 (1964) .
- [15] B. K. Choi, M. N. Lee, and J. J. Kim, *J. Raman Spectrosc.*, **20**, 11 (1989).
- [16] J. M. Winand, A. Rulmont, and P. Tarte, *J. Solid State Chem.*, **87**, 83 (1990).